Available online at www.sciencedirect.com

ScienceDirect

Procedia Engineering 133 (2015) 420 – 432

Procedia Engineering

www.elsevier.com/locate/procedia

6th Fatigue Design conference, Fatigue Design 2015

Comparative study of FE-models and material data for fatigue life assessments of welded thin-walled cross-beam connections

Yevgen Gorash*, Tugrul Comlekci, Donald MacKenzie

Department of Mechanical & Aerospace Engineering, University of Strathclyde, James Weir Building, 75 Montrose Street, Glasgow G1 1XJ, UK

Abstract

This paper investigates the effects of fatigue material data and finite element types on accuracy of residual life assessments under high cycle fatigue conditions. The bending of cross-beam connections is simulated in ANSYS Workbench for three different combinations of structural member shapes: RHS-RHS, RHS-angle and RHS-Channel. The weldments are made of the structural steel grades C350LO and C450LO according to the Australian Standard AS3678. The stress analysis of each weldment having specific profile dimensions under specific cyclic loading is implemented using solid and shell elements considering linear material and geometric response. The stress results are transferred to the fatigue code nCode DesignLife for the residual life prediction. For both variants of FE-mesh, the nominal stress in the weld toes is extracted by splitting the total stress into membrane and bending components and filtering out non-linear component. Considering the effects of mean stress, bending and thickness according to BS7608, failure locations and fatigue life are predicted using the Volvo method and stress integration rules from ASME Boiler & Pressure Vessel Code. Three different pairs of S-N curves (stiff for pure tension and flexible for pure bending) are considered in this work including generic seam weld curves from nCode DesignLife and FE-Fatigue and curves for the Japanese steel JIS G3106-SM490B, which is an equivalent with properties in between C350LO and C450LO. The numerical predictions are compared to the available experimental results highlighting the most preferable fatigue data input and FE-model formulation.

Peer-review under responsibility of CETIM
Keywords: Beams; cyclic loading; fatigue; Finite Element Analysis; steel; Volvo method; welded joints

Nomenclature

SHS	square hollow section	σ_y	yield strength	Ω	bending ratio
RHS	rectang. hollow section	σ_u	ultimate tensile strength	t	component thickness
CA	corner angle	E	elastic modulus	t_{ref}	reference thickness
CC	corner channel	ν	Poisson's ratio	n	thickness exponent
FEA	Finite Element Analysis	$\Delta\sigma$	nominal stress range	k_{tb}	strength correction factor
BCs	boundary conditions	σ_{max}	max. nominal stress	$I_{\Delta\sigma}$	stress range intercept
WDF	weld definition file	N_*	number of cycles	b	fatigue strength exponent

* Corresponding author. Tel.: +44 790 9780901; Fax: +44 141 5520775.
E-mail address: yevgen.gorash@strath.ac.uk

Peer-review under responsibility of CETIM
doi:10.1016/j.proeng.2015.12.612

1. Introduction

Connection by welding is the most effective fabrication process, which is used for a relatively fast manufacturing of big assemblies using simple structural members. Welded joints between metal parts are produced by causing fusion, which includes melting the the base metal and adding the filler material. The phase transformation of a quite small amount of the structural material may usually result into significant residual stresses, heat effected zone with weaker mechanical characteristics, and various welding defects (cracks, distortion, inclusions, incomplete penetration, etc.). In general, such a nature of the welding process means that weldments have a lower fatigue strength than the base material of the parts, which are joined together. The negative effect of welding on the integral strength of the structure is usually minimised during the design process. Any sort of joints including welded need to be kept away from the highly stressed areas, since they increase a stress even more. An infinite fatigue life can be theoretically provided for the base material by identification of the fatigue strength limit, which can be used as a stress limit in the design analysis. Thus, by a proper positioning of weldments the main loading can be carried out primarily by the base material providing an infinite fatigue life. However, even in a well-designed structures, where the weldments are placed away from the load path, the fatigue failures are typically found in weldments [1]. Therefore, the residual life prediction for welded structure should be based in the first instance upon fatigue analysis of weldments.

The fatigue behaviour of weldments has been studied in terms of the geometry of the members, the stresses to which they are subjected, and the materials of which they are fabricated [2]. In regard to the choice of base material, there are a few experimental observations, which may explain its relation to the fatigue strength of corresponding weldments. Initially, when steels of widely differing grades are welded, the resulting S-N curves tend to fall within a single scatter band. The principal reason for this is that superior fatigue strength of high-strength steels as base material is eliminated by the high residual stresses in welds, which may usually approach a yield strength. This idea is discussed by Bonnen *et al.* [3] on example of spot weld load-life curves for mild, moderate and hard steels. However, closer examination of the fatigue curves slopes reveals that low-strength steels (with lower σ_u) tend to have better fatigue resistance in long-term domain under low loads while high-strength steels (with higher σ_u) tend to have better fatigue resistance in short-term domain under high loads. This tendency is confirmed by Ho *et al.* [4] with comparison of fatigue resistance for flame-cut specimens made of two structural steels – A572 (moderate) and A514 (hard). Referring to Palmer [5], it is important to remember that the fatigue life of welded structures is independent of material strength. Moreover, in some cases, structural steels such as grade A514 (hard) prove to be less fatigue resistant than lower-strength steels like A36 (mild). Palmer [5] explains this effect by difference in weldability of these materials (A514 is more difficult to weld than A36). In fact, all these observations show that the fatigue strength of weldments is not completely independent of the base material strength, it is rather inversely proportional to the σ_u of the base material. Therefore, provision of more specific S-N curves for different groups of steels (e.g. mild, moderate and hard) may increase the quality of fatigue assessments. This paper addresses the comparison of specific S-N curve and generic S-N curves for investigation of accuracy of residual life predictions for welded structures.

The most effective way of fatigue assessment is a postprocessing of FEA results of a structural analysis in the form of stress / strain fields (geometry input) in combination with input of load history and fatigue material data. Very basic tools for fatigue life prediction are available in FEA add-ins for advanced CAD products, such as PTC Creo® Simulate and SolidWorks® Simulation. More advanced features of high- and low-cycle fatigue using both stress- and strain-life approaches are supported in specific codes, which are implemented as stand-alone postprocessors and / or modules of commercial FEA software. The leading advanced codes for fatigue analysis available on market and their capabilities are discussed by Chang [6], among them are:

- nCode DesignLife™, which is available as stand-alone product developed by HBM-nCode and module integrated into ANSYS® Workbench environment;
- FE-SAFE™, which is available as stand-alone product developed by Safe Technology Ltd and module integrated into ABAQUS® SIMULIA environment;
- MSC Fatigue® developed by HBM-nCode in conjunction with MSC Software is a part of MSC product line;
- FEMFAT postprocessor is compatible with many of the most commonly used CAE programs;
- Fatigue Module integrated into COMSOL Multiphysics®, etc.

The fatigue code nCode DesignLife embedded in ANSYS Workbench 15 has been chosen for this study, since a number of advanced features have been implemented in it to facilitate the effective fatigue analysis of welds. The

main methods implemented in nCode DesignLife with theoretical background on fatigue of welds and validation cases are outlined in [1,7]. This paper presents a numerical comparative study in order to validate not only available analysis facilities for models in solid and shell formulation, but also the significance of fatigue material data input.

The experimental studies of welded thin-walled cross-beam connections under cyclic bending by Mashiri *et al.* [8–12] have been chosen for this numerical study because of the following features of those experiments:

- Availability of well-documented experiment description, including loads, BCs and fatigue life duration;
- Thin-walled type of geometry of the welded beams, which can be modelled by both solid and shell FEs;
- Complex geometry of the weld seams connecting the beams, which is quite challenging for accurate modelling and prediction of failure location, because it contains the contact of welded components inside the weldment;
- Wide range of applied loads covering domains of moderate and long-term strength from $1 \cdot 10^5$ to $7 \cdot 10^6$ cycles;
- Typical grade of the weldable structural steel with several equivalents available in different national standards is used as material of structural members.

2. Fatigue properties of weldments

The specimens in experiments [8–12] were manufactured from cold-famed high-strength steel of grades C350LO (σ_y = 350 MPa and σ_u = 430 MPa) and C450LO (σ_y = 450 MPa and σ_u = 500 MPa) according to the Australian Standard **AS3678**. These two grades represent the lower (Grade C350) and upper (Grade C450) bounds of the big international group of high-strength structural steels, which includes the following grades:

- *Grade 50 (A, B, C, D)* from British Standard **BS4360**;
- *St52-3* from German Standard **DIN17100**;
- *G3106-SM490 (A, B, C, YA, YB)* from Japanese Standard **JIS**;
- *Fe510 (B, C, D)* from International Standard **ISO630**;
- *A572-345 (-415)* from American Standard **ASTM**;
- *S355 (JR, J0, J2G3, J2G4)* from European Standard **EN10025**.

These all steels are roughly equivalent in chemical composition and have similar elastic properties with elastic modulus of $E = 2 \cdot 10^5$ MPa and Poisson's ratio of $\nu = 0.3$. Since specific fatigue curves for the weldments made of grades C350 or C450 are unavailable in the nCode DesignLife material database, an equivalent fatigue data input is required. The principal aspect in fatigue of weldments is availability of the appropriate experimental data for a long-term strength domain. The most suitable fatigue datasets of this kind are provided by National Institute for Materials Science (Tsukuba, Japan) for the Japanese equivalent from the list above – steel SM490B. The datasets are presented by 5 NIMS Fatigue Data Sheets [13] in 5 parts for cruciform weldments of 5 different thicknesses (9 mm, 20 mm, 40 mm, 80 mm, 160 mm), stress ratio $R = 0$ and duration of tests up to 10^8 cycles, which are illustrated in Fig. 1.

An advantage of nCode DesignLife as a fatigue postprocessor in the availability of effective approaches for fatigue analysis of weldments in both shell and solid elements formulations. The important feature of these approaches is that they are relatively non-sensitive to the quality of finite element mesh. The "Volvo" Method [14] developed at Chalmers University at the behest of Volvo Car Corporation is used for coarse shell models modelled predominantly with 4-node elements. This is a software-friendly method suitable for making FE-based fatigue assessments of welded joints in typical engineering structures, subject to complex loadings, with the minimum of user intervention being required [1]. The method as implemented in software is described in detail in the nCode DesignLife Theory Guide [7]. The method enables a convenient weld modelling approach, since no weld classification is required for input. In case of shell model, only identification of welds as fillet or overlap joints and placing the weld elements in suitable groups or property sets is necessary. The structural stresses at the weld toe, used as an input, are considered as a combination of membrane and bending stresses. They are extracted from the middle of element edge on the weld line using the linear stress field obtained from structural analysis.

In case of solid model formulation, the appropriate elements for analysis can not be automatically identified. Weld fatigue analysis in application to the solids requires more efforts compared to shells as discussed in in nCode documentation [1,7]. The key element of this approach is the stress integration method proposed in ASME BPVC Code [15], when the stress is extracted at several points through thickness, and then extrapolated to produce membrane and bending components. However, the most affords here are demanded by the definition of the weld toe geometry, since the through-thickness integration is automated. A series of points along the weld toe need to be defined, together

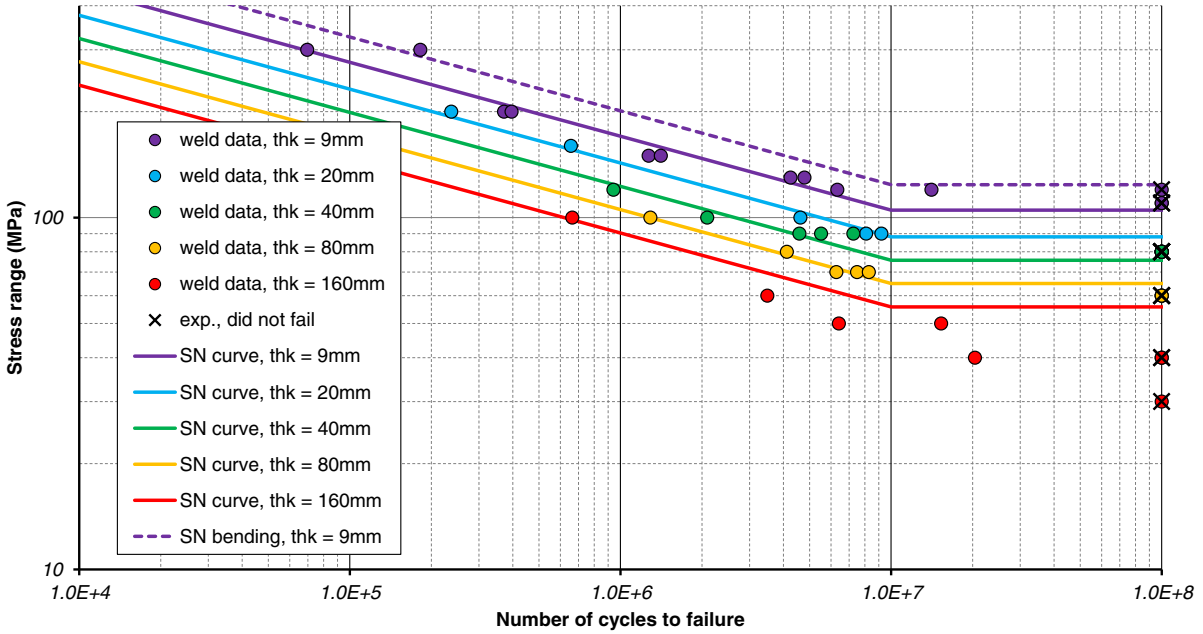

Fig. 1. Experimental and fitted S-N curves of cruciform welded joints made of SM490B steel for different thicknesses [13]

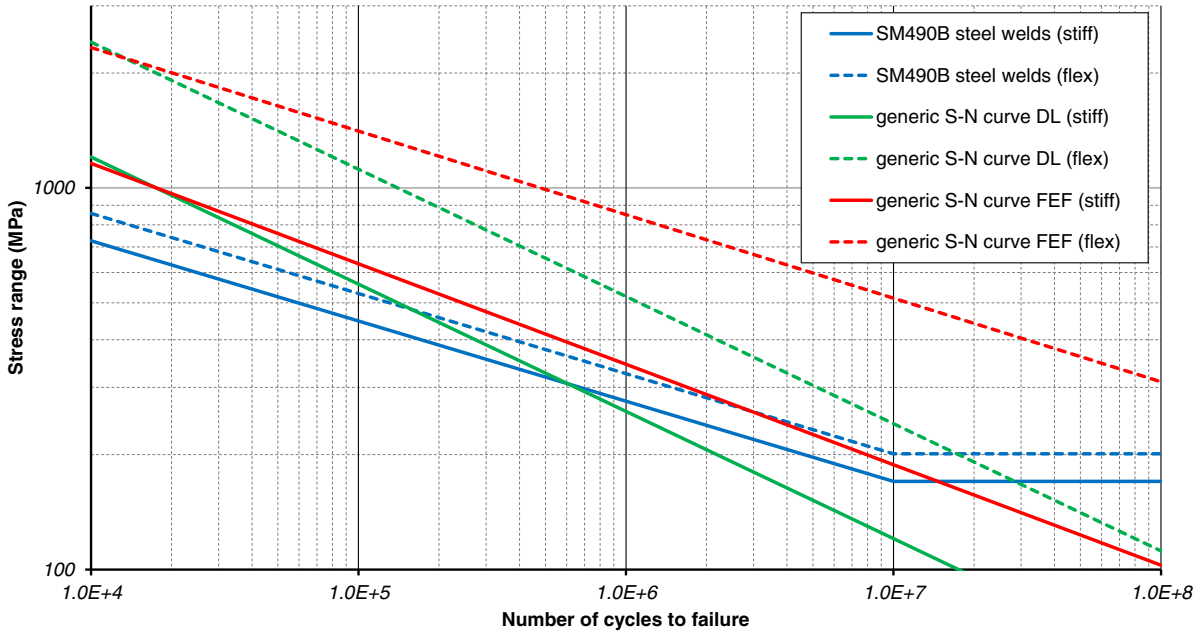

Fig. 2. Three pairs of S-N curves, which are used in weldments fatigue analysis, for 1 mm thickness of welded structures

with a surface normal and another vector to define the orientation of the weld. These points may be defined and imported using an ASCII file in XML format called Weld Definition File (WDF). Currently, tools for creation of this file are not yet released, but they are in development by different CAE vendors. Therefore, in this study coordinates of the weld toe points together with two vectors were measured in SolidWorks using the solid CAD geometry and available internal tools, and then processed in MS Excel spreadsheet to output the WDF.

Table 1. Fatigue constants for three variants of the material, different types of amplitude and values of the reference thickness t_{ref}

material	No.	amplitude	t_{ref} (mm)	n	bending	SRI (MPa)	b
SM490B steel welds	1a	CA	9	0.22	stiff	3100	0.21
					flex	3658	0.21
	1b	CA	1	0.22	stiff	5027	0.21
					flex	5932	0.21
generic SN curves from nCode DL	2a	VA	1	0.16667	stiff	18000	0.3333
					flex	36000	0.3333
	2b	CA	1	0.16667	stiff	25960	0.3333
					flex	51920	0.3333
generic SN curves from nCode FEF	3a	VA	3	0.16667	stiff	8569	0.2632
					flex	11478	0.219
	3b	CA	3	0.16667	stiff	13090	0.2632
					flex	17534	0.219
	3c	CA	1	0.16667	stiff	13090	0.2632
					flex	17534	0.219

An essential feature of fatigue analysis is the mean stress effect, which is also needs to be considered. Weld fatigue assessment includes a mean stress correction using the FKM approach [16], in which the mean stress sensitivity is defined in 4 regimes, with the following slope coefficients [1,7]: $M_1 = 0$, $M_2 = -0.25$, $M_3 = -0.1$ and $M_4 = -0.1$. Another important effect is related to the deformation mode, which is decomposed on bending and tension. The results of extensive testing [14] indicate that the fatigue strength is significantly greater for "flexible" joints where the stresses are predominantly as a result of bending as opposed to "stiff" joints where the majority of the contribution comes from membrane stresses. In both shell and solid formulations, the importance of bending ratio is crucial, and it is defined as the fractional contribution of bending to the overall stress:

$$\Omega = \frac{|\sigma_b|}{|\sigma_b| + |\sigma_n|}. \tag{1}$$

Weld fatigue performance is described by a pair of S-N curves which represent the fatigue strength of a weld under pure membrane (stiff) and bending (flexible) loading conditions. An interpolation is made between the curves based on the bending ratio Ω at each calculation point. Related to the bending is the thickness effect, which is characterised by thicknesses of the welded base material components, and included in fatigue analysis according to the British Standard BS7608 [17]. If a reference thickness is exceeded, the fatigue strength is reduced by a correction factor:

$$k_{tb} = \left(\frac{t_{ref}}{t}\right)^n \left[1 + 0.18\,\Omega^{1.4}\right], \tag{2}$$

where t – thickness of the welded components, t_{ref} – reference thickness, n – thickness exponent.

In notation (2), the fatigue strength increases with increasing bending component (defined by bending ratio Ω) for a decreasing stress range gradient through the thickness. However, the design S-N curves relate to applied loading conditions that produce predominantly membrane stresses. So the S-N curve corresponding to pure bending condition can be obtained from a basic membrane S-N curve by setting the bending ratio $\Omega = 1$. The potentially detrimental effect of increased thickness but beneficial effect from applied bending are combined by the application of the correction factor k_{tb} using Eq. (2) to the stress ranges $\Delta\sigma_b$ obtained from the relevant basic S-N curve [17]:

$$\Delta\sigma = k_{tb}\,\Delta\sigma_b, \tag{3}$$

where $\Delta\sigma$ is a nominal stress range in the structural component under consideration of bending and thickness correction. The basic S-N curve is fitted using the standard nCode DesignLife definition, where the curve consists of 3 linear segments on a log-log plot. The central and long-term domains are defined by the formula [7]:

$$\Delta\sigma_b = \begin{cases} I_{\Delta\sigma 1}\, N_*^{-b_1} & \text{if} \quad N_* < N_{C1} \\ I_{\Delta\sigma 1}\, N_{C1}^{(b_2-b_1)}\, N_*^{-b_2} & \text{otherwise} \end{cases}, \tag{4}$$

where N_* – number of cycles to failure; $I_{\Delta\sigma 1}$ – stress range intercept (MPa); b_1 – first fatigue strength exponent; N_{C1} – transition life; b_2 – second fatigue strength exponent. Transition life N_{C1} defines the point on the curve, where it transitions to the second slope b_2. If b_2 is set to zero, this acts as a fatigue limit.

The experimental data [13] for steel SM490B welds with $t_{\text{ref}} = 9$ mm and stress ratio $R = 0$ is fitted with Eq. (4) producing the constants set No. 1a for constant amplitude (CA) listed in Table 1 with additional constants for long-term domains as $b_2 = 0$ and $N_{C1} = 10^7$, as recommended in BS7608 [17]. The result of fitting with Eq. (4) is illustrated in Fig. 1 with solid blue line. The result of bending correction for $\Omega = 1$ using Eqs (2) and (3) is shown with the dashed blue line. The result of thickness correction using Eqs (2) and (3) is shown with solid lines for thicknesses 20, 40, 80, 160 mm. Since $t_{\text{ref}} = 9$ mm for the constants set No. 1a, it produces very conservative fatigue life predictions for the welded components with $t < 9$ mm. Thus, the constants need to be extrapolated up to $t_{\text{ref}} = 1$ mm to become suitable for fatigue analysis of structural members used in experiments by Mashiri *et al.* [8–12] having thicknesses as $t = 1.4$ mm; 3 mm and 4 mm. This transformation is done combining Eqs (2)-(4) as

$$I^t_{\Delta\sigma 1} = I_{\Delta\sigma 1} \left(t_{\text{ref}} \,/\, t^{new}_{\text{ref}} \right)^n , \tag{5}$$

where t^{new}_{ref} is a new reference thickness and $I^t_{\Delta\sigma 1}$ is a new corresponding stress range intercept. Using the value of $t^{\text{new}}_{\text{ref}} = 1$ mm in Eq. (5), the constant set No. 1a is transformed into the constant set No. 1b, which is listed in Table 1 and illustrated in Fig. 2 with solid and dashed blue S-N curves. This constants set is used in nCode DesignLife for the fatigue analysis of weldments as a specific user fatigue data input characterising the material of weldments.

The advantage of specific fatigue data input needs to be confirmed by comparing it to the generic S-N curves for seam welds for a range of structural steels available in the nCode products databases. DesignLife material database contains a pair of generic S-N curves with the standard slope of 3, $t_{\text{ref}} = 1$ mm and constants given in Table 1 under No. 2a for the assumption of variable amplitude (VA). This assumptions means that $N^{CA}_* = 3\, N^{VA}_*$, because the quality of production is not as good as specimens resulting into Miner's sum effectively reducing to $1/3$. In mathematical terms transformation from VA to CA is expressed in increase of the stress range intercept as

$$I^{CA}_{\Delta\sigma 1} = I^{VA}_{\Delta\sigma 1} \, (1/3)^{-b_1} , \tag{6}$$

where $I^{CA}_{\Delta\sigma 1}$ and $I^{VA}_{\Delta\sigma 1}$ are the stress range intercepts for CA and VA correspondingly. Using Eq. (6), the constant set No. 2a for VA is transformed into the constant set No. 2b for CA, which is listed in Table 1 and illustrated in Fig. 2 with solid and dashed green S-N curves. This constants set is used in nCode DesignLife for the fatigue analysis of weldments as a generic fatigue data input.

Another generic fatigue data input considered in this works is the a pair of generic S-N curves for seam welds from nCode FE-Fatigue, a legacy fatigue postprocessor, predecessor of DesignLife. These S-N curves are described by the constants set No. 3a for $t_{\text{ref}} = 3$ mm and VA, which is given in Table 1 and directly preceded the set No. 2a. In order to be compared to the sets No. 1b and 2b, this constants set No. 3a requires a 2-step transformation. Firstly, Eq. (6) is used to do a VA-CA transformation resulting into the set No. 3b. Secondly, Eq. (5) is used to do reduce t_{ref} from 3 mm to 1 mm resulting into the set No. 3c listed in Table 1 and illustrated in Fig. 2 with solid and dashed red S-N curves.

3. FEA-based fatigue assessment of weldments

The specimens in experiments [8–12] had three ends (left bottom and two top supports) constrained using cylindrical coupling to the ground and one end free. This unconstrained right bottom support has an out-of-plane orthogonal displacement w applied cyclicly, which corresponds to a particular nominal stress range $\Delta\sigma$. The values of $\Delta\sigma$ for each experiment having particular cross-beam connection are listed in Table A.3 in Appendix A. Using the stress ratio $R = 0.1$ from the fatigue experiments [8–12], the nominal stress range $\Delta\sigma$ can be transformed into the maximum nominal stress $\sigma_{\max}$ using the following equations:

$$\sigma_{\max} = \sigma_{\text{ave}} + \sigma_{\text{amp}}, \quad \text{where} \quad \sigma_{\text{ave}} = \sigma_{\text{amp}} \frac{1+R}{1-R} \quad \text{and} \quad \sigma_{\text{amp}} = \frac{\Delta\sigma}{2}, \tag{7}$$

where σ_{ave} is an average nominal stress and σ_{amp} is a nominal stress amplitude. The values of $\sigma_{\max}$ listed in Table A.3 are required for the assessment of corresponding out-of-plane displacement w applied to the unconstrained beam end.

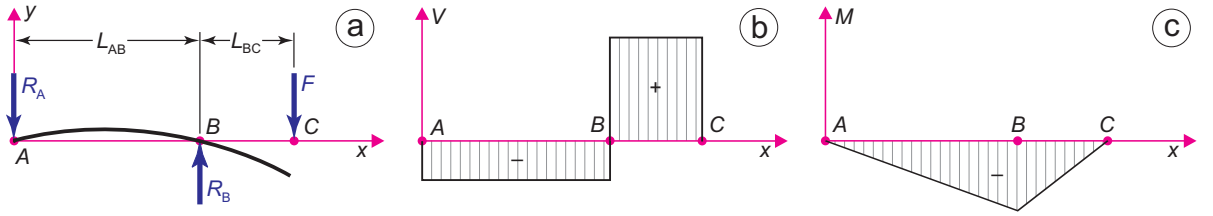

Fig. 3. Diagrams of (a) vertical deflection Y, (b) shear force V, (c) bending moment M for overhanging load applied to simply supported beam [18]

Table 2. Dimensions of 6 variants of the beam cross-sections [mm] according to [19,20] and corresponding area moments of inertia [mm^4]

Square Hollow Sections				Rectangular Hollow Sections	
50x50x3 SHS	50x50x1.6 SHS	35x35x3 SHS	35x35x1.6 SHS	50x25x3 RHS	50x25x1.6 RHS
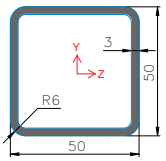	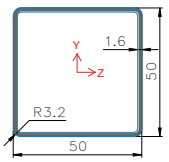	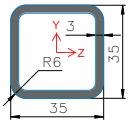	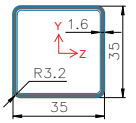	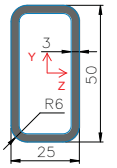	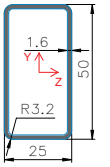
194671.36	117050.41	59483.1	37886.23	111721.36	70182.15

For the assessment of w value, the case of overhanging load applied to simply supported beam, which is available in [18] and illustrated in Fig. 3, is used as a structural equivalent to the cross-beam connection. In this case, locations A and B on a beam from the simplified model are simply supported, and the location C has the orthogonal force applied to it. In experiments [8–12], location A corresponds to the left constrained end of the bottom beam, location B – toe of the weld connecting the beams, and location C – right unconstrained end of the bottom beam. The analytical solution for overhanging load applied to simply supported beam is provided in [18] including equations and corresponding diagrams for vertical deflection Y, shear force V and bending moment M, which are shown in Fig. 3. The most relevant for this study is the equation for deflection of the beam in location C, which is further used as w:

$$Y_C = -\frac{F\,L_{BC}^2\,(L_{AB}+L_{BC})}{3\,E\,I_Z}, \tag{8}$$

where E is an elastic modulus for the material of beam taken from Sec. 2, and I_Z is an area moments of inertia [mm^4] about the neutral axis Z for the beam cross-section. The particular values of I_Z for six variants of the beam profiles for the bottom member are reported in Table 2. These values are calculated using the real geometry of beam profiles in CAD-software SolidWorks with dimensions from Australian / New Zealand standard [19] and technical specification [20], which are shown in Table 2. The beam profile is considered to be located in $Y-Z$ plane with the neutral axis Z going through the profile centre. Therefore, a beam representing the bottom member bends around the axis Z.

In notation (8), the applied bending force F is estimated using the assumption of maximum bending stress being the maximum nominal stress σ_{max} in experiments. Referring to the design guide [21], in experiments [8–12] the nominal stress is caused by the basic load, which was the "bending moment in the bottom member". So the bending force F is obtained from the classic formula for determining the maximum bending stress in the outermost layer of the beam under simple bending:

$$\sigma_{max} = \frac{M\,H_Y}{I_Z} = \frac{F\,L_{BC}\,H_Y}{I_Z} \quad\Longrightarrow\quad F = \frac{\sigma_{max}\,I_Z}{L_{BC}\,H_Y}, \tag{9}$$

where M is the moment about the neutral axis Z and H_Y is the perpendicular distance from the outermost layer of the beam to the neutral axis Z, which in this case corresponds to the half height of the section profile indicated in Table 2.

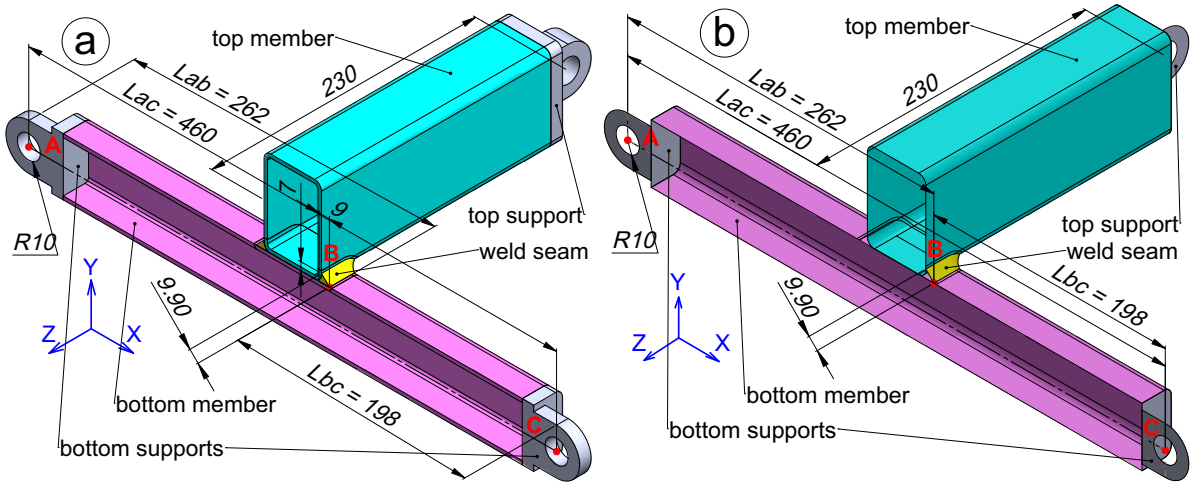

Fig. 4. Geometry, components definition and dimensions (mm) for 75x50x3 RHS to 50x50x3 SHS connection using (a) solids and (b) surfaces

Equations (8) and (9) are used to estimate the values of w corresponding to σ_{max} with additional input of parameters specific for each experiment like I_Z, L_{AB} and L_{BC}. The resultant values of the displacement w, which is applied to the right end of bottom member, are reported in Table A.3 in Appendix A.

The comprehensive geometrical models of welded cross-beam connections were created in CAD-software SolidWorks in solids and surfaces presentation including top and bottom members, top and bottom supports, and the weld seam. The dimensions of beam profiles are taken from Australian / New Zealand standard [19] and technical specification [20]. All variants of tubes (RHS/SHS), angles (CA) and channels (CC) are listed in Table A.3. It should be noted that the specimens geometry can be simplified only to a half (not a quarter) using the vertical symmetry plane along the bottom member, because of the unsymmetric loading. The example of the geometry for the connection of 75x50x3 RHS (top member) to 50x50x3 SHS (bottom member) is shown in Fig. 4a using solids and in Fig. 4b using surfaces. The distance between centres of supports in this work is assumed to be 460 mm. In accordance to the 2D model of a simply supported beam in Fig. 3, the points A, B and C are denoted in Fig. 4. The legs of welds around the rounded corners are 9 mm (horizontal) and 7 mm (vertical) giving 8 mm in average in compliance with experiments [12]. The weld face length is 9.9 mm, and the weld throat considered in shell model formulation is 6 mm.

The most tricky point in preparation of the specimen geometry for FEA is the merging of the weld seam with top and bottom members, while keeping the zero gap between the beams to account for contact separation. In case of shell FE-mesh this operation is done simply using the mesh connection feature, which merges the adjacent nodes of the weld seam and beams during the mesh generation. In case of solid FE-mesh this operation requires more efforts in geometrical preprocessor of ANSYS Workbench – Geometry Modeller. The Connection operation needs be used to merge the adjacent surfaces of the weld seam and beams, while avoiding any merging between the the adjacent surfaces of the beams. In both shell and solid FE-models, such sort of geometry preparation results in a single FE-mesh with naturally a crack (zero gap) in a small area between the beams, which is surrounded by the weld seam. For a realistic behaviour of the structural deformation, this location hidden inside the weldment is modelled by the frictionless contact feature with all default settings. The example of the FE-mesh corresponding to the configuration 75x50x3 RHS to 50x50x3 SHS, together with mesh statistics and blowup of the location of contact between the beams are shown in Fig. 5a using solid FEs and Fig. 5b using shell FEs. It should be noted that the solution of the shell model is performed much quicker than the solution of the solid model since the number of solved equations expressed in the number of nodes is 3 times smaller in shell model.

In solid model, a cylindrical type of constrain is applied to 3 constrained supports, which assumes 1 rotational degree of freedom (DOF) around the longitudinal axis and 1 translational DOF along the same axis. In shell model, the same boundary conditions applied to same 3 supports are simulated by constraining 2 in-plain displacements (equivalent to constraining the radial displacement) and constraining 2 out-of-plain rotations, which are constrained in cylindrical coupling. This results in only 2 DOFs in each of 3 supports and the vertical displacement applied to the

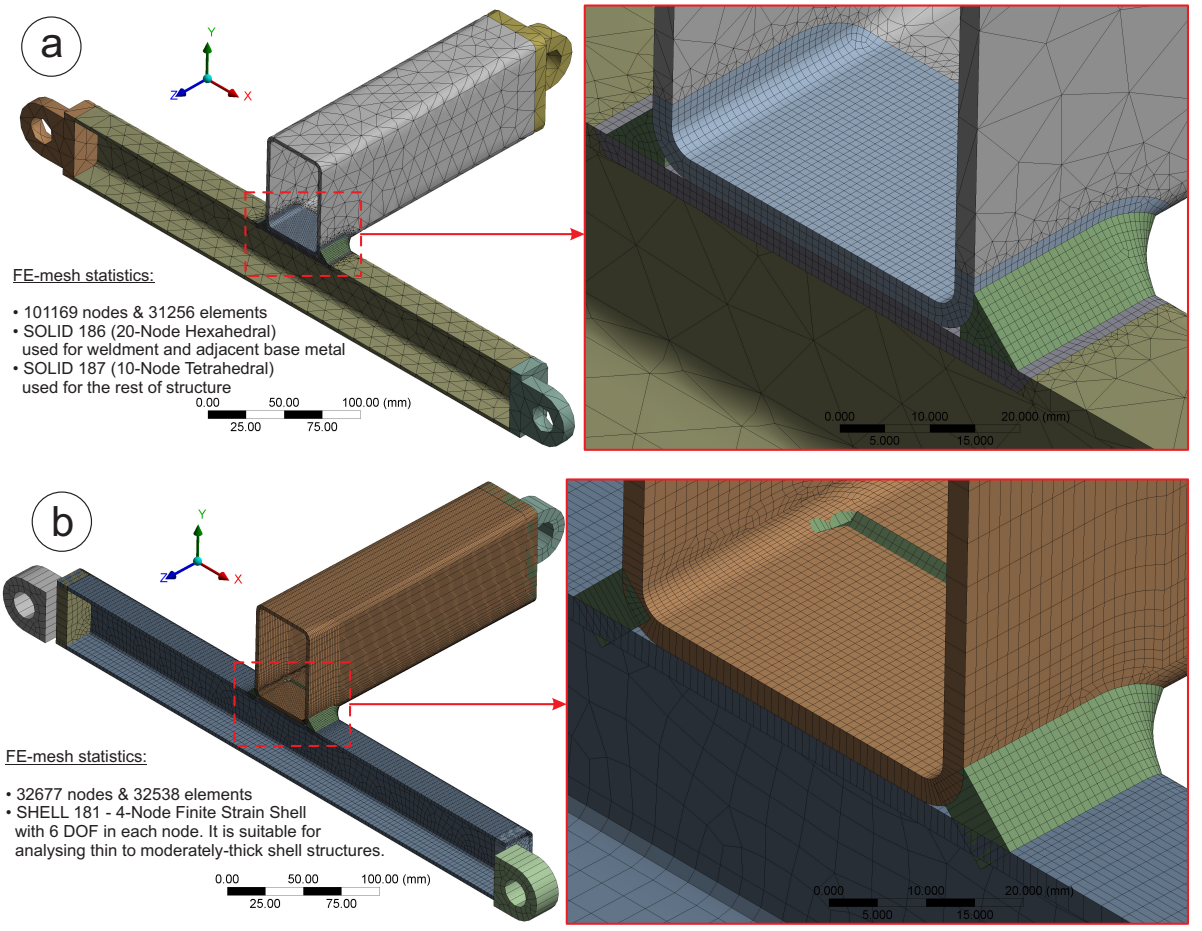

Fig. 5. FE-mesh, statistics and blowup of the weldment area for 75x50x3 RHS to 50x50x3 SHS connection using (a) solid FEs and (b) shell FEs

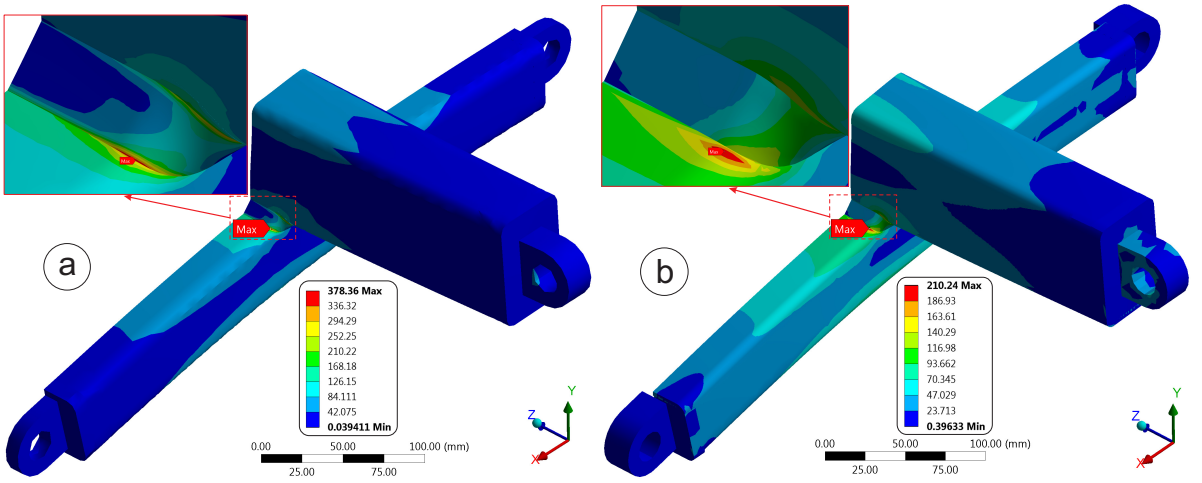

Fig. 6. Equivalent von Mises stress (MPa) for 75x50x3 RHS to 50x50x3 SHS connection for (a) solid FE-model and (b) shell FE-model

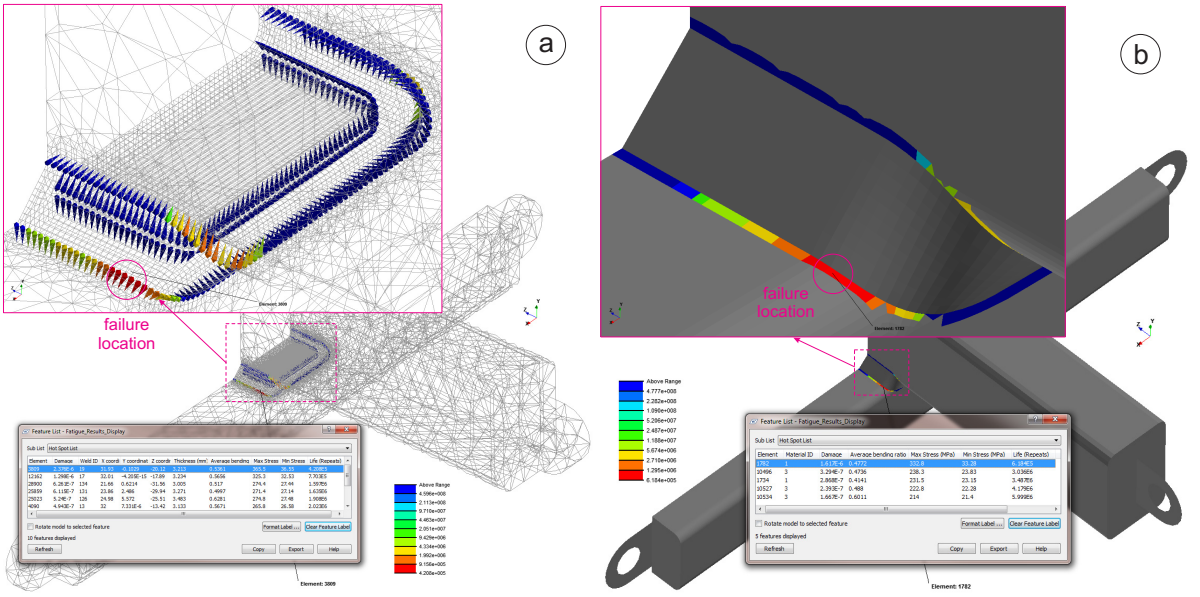

Fig. 7. Result of fatigue life predictions (cycles) for 75x50x3 RHS to 50x50x3 SHS connection for (a) solid FE-model and (b) shell FE-model

centre of 4th support directed downwards. With absolutely equivalent BCs and loads applied to the shell and solid FE-models, the maximum values of equivalent von Mises stress obtained in result of structural analyses are about twice different. The examples of stress distribution together with blowup of the area of the highest stress are shown in Fig. 6a using solid FEs and in Fig. 6b using shell FEs. Such a difference in maximum stress values is explained by the assumption that shell FE-model output a maximum hotspot stress in vicinity of the weld toe, while the maximum stress in solid FE-model is contributed by a non-linear component of stress caused by geometrical singularity.

4. Discussion

The results of fatigue life predictions are obtained for shell formulation for 3 variants of cross-beam connections: <1> tube [RHS] to tube [RHS/SHS], <2> angle [CA] to tube [RHS/SHS], and <3> channel [CC] to tube [RHS/SHS]. Three variants of fatigue data input for CA and $t_{\text{ref}} = 1$ mm reference thickness are used in predictions: <1> S-N curves of SM490B steel welds, and generic S-N curves from <2> nCode DesignLife and <3> nCode FE-Fatigue). The examples of fatigue life predictions for the connection of 75x50x3 RHS to 50x50x3 SHS beams together with blowup of the crack location are shown in Fig. 7a using solid FEs and in Fig. 7b using shell FEs. The advantage of all performed numerical predictions is that the crack has been predicted exactly in the same location as in experiments [8–12] – front part of the weld toe on the fillet of the bottom member. The numerical predictions N_*^{FE} are compared to the experimental fatigue life N_*^{exp} in Table A.3 using the following formula for discrepancy in percents %:

$$\Delta N_* = \frac{100\ (N_*^{exp} - N_*^{FE})}{\min(N_*^{exp}, N_*^{FE})}. \tag{10}$$

This value characterises not only relative deviation, but also the amount of conservatism is defined by the sign of this value: positive – conservative and negative – non-conservative. The total value of discrepancies are calculated for three groups of experiments (RHS-RHS/SHS, CA-RHS/SHS, CC-RHS/SHS) – these and aggregate values for all considered experiments are reported in Table A.3.

Two experiments in the test group <1> are not considered for calculation of summary discrepancies as denoted in Table A.3 by grey background. Test S5R1L1A is ignored, because the discrepancies for all three materials are too much different from from the rest of the tests. As an assumption, there could be something wrong with reported conditions of this test in [11]. Test R2R1L1A is ignored, because no failure was found after 7738790 cycles. However, the result obtained with the S-N curves <1> is the most preferable, because no failure was identified in this simulation.

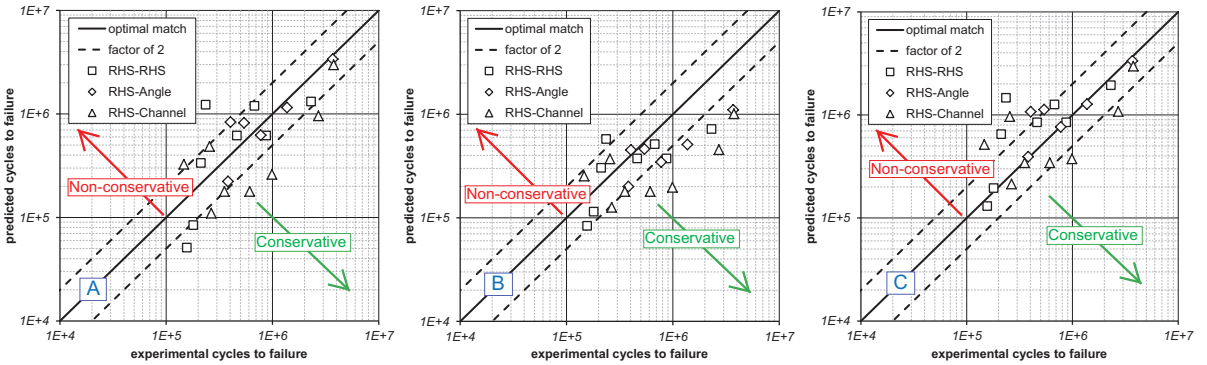

Fig. 8. Comparison of the observed and predicted cycles to failure using shell elements for: a) S-N curves for SM490B steel welds; b) new generic S-N curves in nCode DesignLife c) old generic S-N curves in nCode FE-Fatigue

In the test group <1> the S-N curves <1> produce the best overall result (-158.91%) regardless of its non-conservatism, because its discrepancy is the smallest compared to the results produced with S-N curves <2> (360.70%) and <3> (-869.95%). In the test group <2> the S-N curves <1> produce even better overall result (-34.05%) also with a non-conservatism – its discrepancy is much smaller than the discrepancies produced with S-N curves <2> (624.67%) and <3> (-258.59%). However, in the test group <3> the best overall discrepancy is produced by the S-N curves <3> (-80.97%) again with a non-conservatism as opposed to other two results, where the discrepancies produced with S-N curves <1> (760.59%) and <2> (1505.96%) are conservative.

Total aggregate discrepancies for all considered experiments reveal the winner – S-N curves <1> of SM490B steel welds with slightly conservative result of 25.80%. It is more preferable to a much more conservative result of 113.24% produced by generic S-N curves <2> from nCode DesignLife and to a non-conservative result of -54.98% produced by generic S-N curves <3> from nCode FE-Fatigue. Obtained results for mathematical assessment of the failure prediction quality using Eq. (10) comply very well with a graphical representation of comparison of the observed and predicted cycles to failure in Fig. 8. Predictions with S-N curves <1> are the most balanced about the diagonal of optimal match with only 5 predictions being out of the domain for factor of 2. Predictions with S-N curves <2> are accurate for the $N_* < 10^6$, but very conservative for long fatigue life durations with $N_* > 10^6$. Predictions with S-N curves <3> are accurate for long fatigue life durations with $N_* > 10^6$, but very non-conservative for $N_* < 10^6$.

The total discrepancy of fatigue life predictions obtained using solid formulation haven't been examined in this work, since they are much more time consuming than analyses with shell elements. In addition to higher computational costs, solid elements approach requires a Weld Definition File (WDF), which takes the most efforts to be generated. In this work, the procedure for a partly automatic generation of the WDF is implemented using SolidWorks and MS Excel, but preparation of WDF is still durational. Nevertheless, 3 different variants of cross-beam connection have been examined with the bottom member 50x50x3 SHS welded to the top member being either 75x50x3 RHS or 75x75x4 CA or 100x50x4 CC. As reported in Table A.4, the predictions with solid FEs are more conservative compared to shell FEs with differences of 35.2%, 14.7% and 18.7% calculated using Eq. (10) and resulting into 22.9% average difference, which is quite satisfactory.

Recently the fatigue analysis in solid formulation has been drastically improved and accelerated with a release of ACT extension for ANSYS Workbench titled nCode Weldline [22]. This new add-in brings a dramatic progress into the analysis of complex assemblies with a free-form geometry and arbitrary location of welded joints. In fact, this is a custom result object for creating a WDF in XML format, which is embedded into the Workbench interface. The generation of WDF is automated and simplified for solid geometry with user input of weld toe edges and base metal surfaces adjacent to selected edges. Therefore, in continuation of this work, all variants of cross-beam connections listed in Table A.3, which have been analysed in this work in shell formulation, will be analysed in solid formulation using the nCode Weldline ACT extension. The channel to channel (CC-CC) variant of connection available in [12] hasn't been included in scope of this work, since its geometry couldn't be simplified using symmetry condition and requires the consideration of whole geometry. Thus, the fatigue analysis of CC-CC connection in both shell and solid formulations is also planned for future work.

Acknowledgements

The authors deeply appreciate the experts of HBM - nCode for the workshops, seminars and comprehensive technical support of their leading product – nCode DesignLife. Particular gratitude is expressed to Jeffrey Mentley for an essential assistance and consultations during the course of this work.

Appendix A. Summary of experiments and simulations

Summary of experiments and simulations including conditions and results of tests, analytical assessments and numerical predictions is reported in Table A.3 for three variants of cross-beam connections: <1> tube (RHS) to tube (RHS/SHS), <2> angle (CA) to tube (RHS/SHS), and <3> channel (CC) to tube (RHS/SHS). Comparison of fatigue life predictions obtained with shell and solid FE-models with each other and experimental data is reported in Table A.4 for cross-beam connections with bottom member 50x50x3 SHS welded to three variants of top members: <1> 75x50x3 RHS, <2> 75x75x4 CA, and <3> 100x50x4 CC.

References

[1] P. Heyes, Fatigue analysis of seam welded structures using nCode DesignLife, Whitepaper, HBM nCode, Rotherham, UK, (Mar. 2013). URL:http://www.ncode.com/fileadmin/mediapool/nCode/downloads/DesignLife/Whitepaper_SeamWelds_nCodeDesignLife_201303-3.pdf.

[2] W. H. Munse, Fatigue of weldments – Tests, design, and service, in: D. W. Hoeppner (Ed.), Fatigue Testing of Weldments (ASTM STP 648), American Society for Testing and Materials, Philadelphia, PA, USA, 1978, pp. 89–112. DOI: 10.1520/STP648-EB.

[3] J. J. F. Bonnen, H. Agrawal, M. A. Amaya, R. M. Iyengar, H. T. Kang, A. K. Khosrovaneh, T. M. Link, H.-C. Shih, M. Walp, B. Yan, Fatigue of advanced high strength steel spot-welds, SAE Technical Paper no. 2006-01-0978 (2006) 1–20. DOI: 10.4271/2006-01-0978.

[4] N.-J. Ho, F. V. Lawrence Jr., C. J. Altstetter, The fatigue resistance of plasma and oxygen cut steel, Welding Research Supplement (Nov. 1981) 231–236. URL: https://app.aws.org/wj/supplement/WJ_1981_11_s231.pdf.

[5] T. Palmer, Fatigue in welded-steel structures, Machine Design (Mar. 3, 2014). URL: http://machinedesign.com/metals/fatigue-welded-steel-structures.

[6] K.-H. Chang, Fatigue and fracture analysis, in: Product Performance Evaluation with CAD/CAE, The Computer Aided Engineering Design Series, Academic Press, Boston, USA, 2013, pp. 205–273. DOI: 10.1016/B978-0-12-398460-9.00004-4.

[7] P. Newbold, DesignLife Theory Guide, Version 9 ed., HBM nCode, Rotherham, UK, 2013.

[8] F. R. Mashiri, X. L. Zhao, Welded thin-walled rhs-to-rhs cross-beams under cyclic bending, in: J. A. Packer, S. Willibald (Eds.), Proc. Tubular Structures XI (Québec, Canada, 31 Aug. - 2 Sep. 2006), Taylor & Francis Group, CRC Press, London, UK, 2006, pp. 97–104.

[9] F. R. Mashiri, X. L. Zhao, Thin RHS-Channel welded cross-beams under cyclic bending, in: J. Y. R. Liew, Y. S. Choo (Eds.), Proc. 5th Int. Conf. in Advances in Steel Structures – ICASS 2007 (Singapore, 5-7 Dec. 2007), Research Publishing Service, Singapore, 2007, pp. 991–996.

[10] F. R. Mashiri, X. L. Zhao, Tests of welded cross-beams under fatigue loading, in: Z. Y. Shen, Y. Y. Chen, X.-Z. Zhao (Eds.), Proc. Tubular Structures XII (Shanghai, China, 8-10 Oct. 2008), Taylor & Francis Group, CRC Press, Boca Raton, FL, USA, 2008, pp. 163–170.

[11] F. R. Mashiri, X. L. Zhao, Fatigue tests and design of welded thin-walled RHS-RHS and RHS-angle cross-beam connections under cyclic bending, Thin-Walled Structures 48 (2010) 159–168. DOI: 10.1016/j.tws.2009.07.006.

[12] F. R. Mashiri, X. L. Zhao, L. W. Tong, Fatigue tests and design of welded thin-walled RHS-Channel and Channel-Channel cross-beam connections under cyclic bending, Thin-Walled Structures 63 (2013) 27–36. DOI: 10.1016/j.tws.2012.09.002.

[13] Data Sheet on Fatigue Properties of Non-Load-Carrying Cruciform Welded Joints of SM490B Rolled Steel for Welded Structure, NIMS Fatigue Data Sheets No. 91, 96, 99, 108, 114, National Institute for Materials Science, Tsukuba, Japan, (2003, 2004, 2006, 2009, 2011).

[14] M. Fermér, M. Andréasson, B. Frodin, Fatigue life prediction of mag-welded thin-sheet structures, SAE Technical Papers (1998) 1–9. DOI: 10.4271/982311.

[15] A. Boiler, P. V. C. on Pressure Vessels, 2010 ASME Boiler & Pressure Vessel Code: Section VIII Division 2 – Alternative Rules, 2010 ed., ASME, New York, USA, 2010.

[16] E. Haibach, FKM-Guideline: Analytical Strength Assessment of Components in Mechanical Engineering, 5th ed., VDMA Verlag, FKM, Frankfurt am Main, Germany, 2003.

[17] British Standard, Guide to fatigue design and assessment of steel products, BS 7608:2014, The British Standards Institution, London, UK, 2014.

[18] R. G. Budynas, J. K. Nisbett, Shigley's Mechanical Engineering Design, 9th ed., McGraw-Hill, New York, USA, 2010.

[19] Australian / New Zealand Standard, Cold-formed structural steel hollow sections, AS/NZS 1163:2009, Standards Australia / Standards New Zealand, Sydney / Wellington, 2009.

[20] AustubeMills, TS100 – angles, channels, flats, DuraGal® Technical Specifications, 7th ed., Australian Tube Mills Pty Ltd., Acacia Ridge, QLD, Australia, 2013.

[21] X.-L. Zhao, S. Herion, J. A. Packer, R. S. Puhtli, G. Sedlacek, J. Wardenier, K. Weynand, A. M. van Wingerde, N. F. Yeomans, Design guide for circular and rectangular hollow section welded joints under fatigue loading, TÜV-Verlag GmbH, Köln, Germany, 2001.

[22] J. Mentley, nCode DesignLife Weldline ACT Extension, PowerPoint Presentation, HBM - nCode Products (Southfield, MI, USA), 2015.

Table A.3. Summary of experiments and simulations including conditions and results of tests, analytical assessments and numerical predictions

Groups	Experimental data for cross-beam connections with different combinations of beam profiles						Analytical assessments		Numerical predictions with nCode DesignLife					
									SM490B steel welds		generic S-N curve DL		generic S-N curve FEF	
	No.	Top	Bottom	$\Delta\sigma_{nom}$	N*	Failure	σ_{max}	w (mm)	N*	Δ, %	N*	Δ, %	N*	Δ, %
Tube to tube	S1R1L1A	75x50x3 RHS	50x50x3 SHS	149.7	871688	bottom member	166.333	1.00998	6.184E+05	40.96	3.747E+05	132.64	8.479E+05	2.81
	S1R1L2A				461734				6.184E+05	-33.93	3.747E+05	23.23	8.479E+05	-83.63
	S2R1L1A		50x50x1.6 SHS	93.5	2304714		103.889	0.63081	1.319E+06	74.73	7.208E+05	219.74	1.942E+06	18.68
	S2R1L2A			124.6	211506		138.444	0.84063	3.362E+05	-58.96	3.046E+05	-44.01	6.522E+05	-208.36
	S4R1L1A		35x35x3 SHS	214.4	156087		238.222	2.06641	5.120E+04	204.86	8.373E+04	86.42	1.307E+05	19.42
	S4R1L2A			193.0	179735		214.444	1.86015	8.448E+04	112.75	1.148E+05	56.56	1.949E+05	-8.44
	S5R1L1A		35x35x1.6 SHS	135.0	1316243		150	1.30114	9.348E+04	1308.05	1.030E+05	1177.91	1.653E+05	696.28
	R2R1L1A		50x25x3 RHS	65.2	7738790	no crack	72.444	0.43988	no crack estimated		4.630E+06	under	2.047E+07	over
	R2R1L2A			130.5	235219	BM	145	0.88044	1.228E+06	-422.07	5.772E+05	-145.39	1.466E+06	-523.25
	R3R1L1A		50x25x1.6 RHS	103.8	675844		115.333	0.7003	1.198E+06	-77.26	5.139E+05	31.51	1.265E+06	-87.17
	Total discrepancy for the above group of tests:									-158.91		360.70		-869.95
Corner to tube	S1AN1L1A	75x75x4 CA	50x50x3 SHS	145.2	540340	bottom member	161.333	0.91777	8.190E+05	-51.57	4.605E+05	17.34	1.128E+06	-108.76
	S1AN1L2A		50x50x1.6 SHS	152.9	381510		169.889	0.96644	2.228E+05	71.23	2.002E+05	90.56	3.924E+05	-2.85
	S4AN1L2A		35x35x3 SHS	87.6	3693392		97.333	0.791	3.380E+06	9.27	1.101E+06	235.46	3.347E+06	10.35
	S5AN1L1A		35x35x1.6 SHS	110.3	775613		122.556	0.99597	6.222E+05	24.66	3.452E+05	124.69	7.642E+05	1.49
	R2AN1L1A		50x25x3 RHS	133.2	403180		148	0.84192	8.329E+05	-106.58	4.520E+05	-12.11	1.075E+06	-166.63
	R3AN1L1A		50x25x1.6 RHS	106.0	1371361		117.778	0.67	1.153E+06	18.94	5.103E+05	168.74	1.272E+06	7.81
	Total discrepancy for the above group of tests:									-34.05		624.67		-258.59
Channel to tube	S1C1L1A	100x50x4 CC	50x50x3 SHS	154.7	353652	bottom member	171.889	1.04371	1.784E+05	98.24	1.791E+05	97.46	3.433E+05	3.02
	S1C1L2A				611060				1.784E+05	242.52	1.791E+05	241.18	3.433E+05	78.00
	S2C1L1A		50x50x1.6 SHS	96.5	255855		107.222	0.65105	4.854E+05	-89.72	3.707E+05	-44.89	9.638E+05	-276.70
	S4C1L1A		35x35x3 SHS	177.2	265871		196.889	1.70787	1.098E+05	142.14	1.261E+05	110.84	2.136E+05	24.47
	S4C1L2A			88.6	3760725		98.444	0.85394	2.980E+06	26.20	1.009E+06	272.72	2.973E+06	26.50
	S5C1L1A		35x35x1.6 SHS	139.5	990477		155	1.34451	2.607E+05	279.93	1.966E+05	403.80	3.747E+05	164.34
	R2C1L1A		50x25x3 RHS	134.8	146712		149.778	0.90945	3.262E+05	-122.34	2.530E+05	-72.45	5.156E+05	-251.44
	R3C1L1A		50x25x1.6 RHS	107.2	2711681		119.111	0.72324	9.561E+05	183.62	4.540E+05	497.29	1.081E+06	150.85
	Total discrepancy for the above group of tests:									760.59		1505.96		-80.97
	Total discrepancy for all considered experiments:									25.80		113.24		-54.98

Table A.4. Comparison of fatigue life predictions obtained with shell and solid FE-models with each other and experimental data

Case No.	Experiments for connection with bottom member 50x50x3 SHS			SM490B steel welds {1}				generic S-N curve DL {2}				generic S-N curve FEF {3}				difference - shell vs. solid			
				shell FEs		solid FEs		shell FEs		solid FEs		shell FEs		solid FEs		{1}	{2}	{3}	total
	No.	Top member	N*	N*	Δ, %	N*	Δ, %	N*	Δ, %	N*	Δ, %	N*	Δ, %	N*	Δ, %	Δ, %	Δ, %	Δ, %	Δ, %
1	S1R1L1A	75x50x3 RHS	871688	6.184E+05	41.0	4.208E+05	107.2	3.747E+05	132.6	2.978E+05	192.7	8.479E+05	2.8	6.386E+05	36.5	47.0	25.8	32.8	35.2
	S1R1L2A		461734		-33.9		9.7		23.2		55.0		-83.6		-38.3				
2	S1AN1L1A	75x75x4 CA	540340	8.190E+05	-51.6	7.175E+05	-32.8	4.605E+05	17.3	4.116E+05	31.3	1.128E+06	-108.8	9.549E+05	-76.7	14.1	11.9	18.1	14.7
3	S1C1L1A	100x50x4 CC	353652	1.784E+05	98.2	1.424E+05	148.4	1.791E+05	97.5	1.573E+05	124.8	3.433E+05	3.0	2.932E+05	20.6	25.3	13.9	17.1	18.7
	S1C1L2A		611060		242.5		329.1		241.2		288.5		78.0		108.4				